

Evaluation for Regression Analyses on Evolving Data Streams

Yibin Sun*

University of Waikato
Hamilton, Waikato, New Zealand
yibin.spencer.sun@gmail.com

Bernhard Pfahringer

University of Waikato
Hamilton, New Zealand
bernhard@waikato.ac.nz

Heitor Murilo Gomes

Victoria University of Wellington
Wellington, New Zealand
heitor.gomes@vuw.ac.nz

Albert Bifet

University of Waikato
Hamilton, New Zealand
abifet@waikato.ac.nz

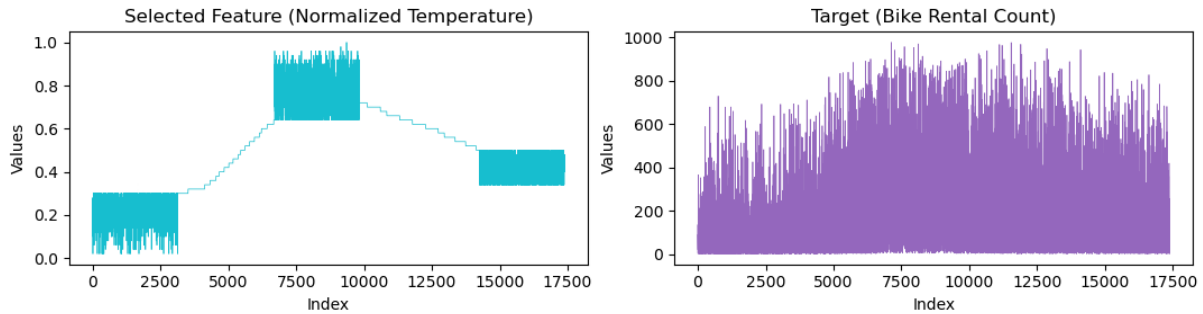


Figure 1: Simple Showcase of Feature and Target Values with Simulated Incremental Drifts

Abstract

The paper explores the challenges of regression analysis in evolving data streams, an area that remains relatively underexplored compared to classification. We propose a standardized evaluation process for regression and prediction interval tasks in streaming contexts. Additionally, we introduce an innovative drift simulation strategy capable of synthesizing various drift types, including the less-studied incremental drift. Comprehensive experiments with state-of-the-art methods, conducted under the proposed process, validate the effectiveness and robustness of our approach.

CCS Concepts

• Information systems → Data stream mining; • Computing methodologies → Supervised learning by regression.

Keywords

Data Streams, Evaluation, Regression, Prediction Interval, Drift Simulation

ACM Reference Format:

Yibin Sun, Heitor Murilo Gomes, Bernhard Pfahringer, and Albert Bifet. 2018. Evaluation for Regression Analyses on Evolving Data Streams. In *Proceedings of Make sure to enter the correct conference title from your rights confirmation email (Conference acronym 'XX)*. ACM, New York, NY, USA, 11 pages. <https://doi.org/XXXXXXXX.XXXXXXX>

1 Introduction

Machine learning on streaming data has garnered significant interest due to its applicability in dynamic and evolving environments [14, 27]. However, while extensive research has focused on classification tasks in stream learning, regression tasks remain underexplored [3], one of the reason is the lack of dedicated data resources [32]. The challenges are further compounded by the difficulty in defining and identifying the drift in the real-world data sequences [34]. A real-world application of data stream regression includes real-time energy pricing adjustments based on evolving market conditions [30]. Additionally, Prediction Intervals (PI) for streaming data have demonstrated significant effectiveness in quantifying regression uncertainty [30].

In this work, we aim to address these gaps by making the following key deliverables: (1) Standardized procedure and metrics for evaluating streaming regression algorithms, (2) Methodologies for simulating concept drifts, especially incremental drifts, (3) Empirical analysis using state-of-the-art streaming regression and prediction interval techniques.

All code, datasets, and scripts are publicly available on GitHub¹, ensuring full transparency and reproducibility. This paper aims

Permission to make digital or hard copies of all or part of this work for personal or classroom use is granted without fee provided that copies are not made or distributed for profit or commercial advantage and that copies bear this notice and the full citation on the first page. Copyrights for components of this work owned by others than the author(s) must be honored. Abstracting with credit is permitted. To copy otherwise, or republish, to post on servers or to redistribute to lists, requires prior specific permission and/or a fee. Request permissions from permissions@acm.org.
Conference acronym 'XX, June 03–05, 2018, Woodstock, NY

© 2018 Copyright held by the owner/author(s). Publication rights licensed to ACM.
ACM ISBN 978-1-4503-XXXX-X/18/06
<https://doi.org/XXXXXXXX.XXXXXXX>

¹<https://github.com/YibinSun/KDD25-DriftSimulation/>

to establish a foundation for rigorous regression research in data streams while encouraging the adoption of open-source practices.

2 Background

This section provides basic introduction to the stream learning concepts relevant to this work.

2.1 Data Stream

Data stream refers to continuous, real-time flow of data that requires dynamic processing and analysis [1]. Typical sources of data streams include sensors, logs, online activities, and etc [23]. Streaming data increasingly grows its significance as the world digitalizing [6].

A data stream usually consist of a sequence of examples $DS = \{X_1, X_2, X_3, \dots, X_t, \dots\}$ that can be mapped to a target sequence $\mathcal{Y} \in \{\mathcal{Y}_1, \mathcal{Y}_2, \mathcal{Y}_3, \dots, \mathcal{Y}_t, \dots\}$, where the subscript t denotes the observation moment (time step). Traditionally, the X is a d -dimensional vector and \mathcal{Y} represents the ground truth at the moment t . In the more explored classification scenario, \mathcal{Y} is usually one of the n possible labels (classes), i.e., $\mathcal{Y} \in \{C_1, C_2, \dots, C_n\}$. However, in this work we focus on the regression tasks, where \mathcal{Y} is a continuous value, i.e., $\mathcal{Y} \in \mathbb{R}$.

It is worth mentioning that the label \mathcal{Y} can be not available all the time. Consequently, stream learning can be categorized into several sets [10]:

- Supervised Learning: where \mathcal{Y} is always immediately available after the observation moment;
- Unsupervised Learning: where \mathcal{Y} is never available;
- Semi-supervised Learning: where \mathcal{Y} is partially available; and
- Delayed Learning: where \mathcal{Y} can be available at any moment posterior to the observation.

This work has a sole concentration on supervised learning. Hence, the regression DS under full supervision can be represented as $DS_s = \{(X_1, \mathcal{Y}_1), (X_2, \mathcal{Y}_2), (X_3, \mathcal{Y}_3), \dots, (X_t, \mathcal{Y}_t), \dots\}$.

Conventional machine learning approaches always encounter issues when applying to streaming data [1]. For instance, due to the potentially infinite amount of data points, data streams cannot be stored in the machine's memory [21]. Moreover, the high arrival velocity of the streaming data strictly restricts the processing time on each instance [4]. The temporal order also raises the crucial phenomenon of concept drift when the underlying distribution of the data shifts over time [2]. These constraints require the streaming algorithms to be efficient enough, can only access to an instance once (or a small amount of times), and be able to detect and adapt to the new distributions in the occurrence of concept drifts.

2.2 Concept Drift

Machine learning typically assumes that the data points are independent and identically distributed (i.i.d.). However, this assumption is frequently violated in stream learning, especially with the drifting concepts. Stream learning further assumes that the data within the a single concept should be i.i.d., yet instances from different concepts violate the i.i.d. assumption [9, 15].

As a consequence, concept drifts can be categorized into different types according to the behaviours when changes occur [7, 15].

Abrupt (Sudden) drift refers to the sudden change from a concept to another one. An abrupt can be expressed as:

$$DS_a = \{X_1^a, X_2^a, X_3^a, \dots, X_t^a, X_{t+1}^b, X_{t+2}^b, X_{t+3}^b, \dots\}$$

where a and b denote different concepts. At moment t , the data suddenly switch its source from concept a to b .

Gradual drift refers to a drift between two concepts with a fluctuation period, which can be formulated as:

$$DS_g = \{X_1^a, X_2^a, X_3^a, \dots, X_t^a, X_{t+1}^b, X_{t+2}^a, X_{t+3}^b, X_{t+4}^b, X_{t+5}^a, \dots, X_{t'}^b, X_{t'+1}^b, X_{t'+2}^b, \dots\}$$

During moment t to $t + 5$, a mixed data from both concept a and b is presented.

Incremental drift refers to a gradual and continuous transition between two concepts over time. This can be formulated as:

$$DS_i = \{X_1^a, X_2^a, \dots, X_t^a, X_{t+1}^{a \rightarrow b}, X_{t+2}^{a \rightarrow b}, \dots, X_{t'}^{a \rightarrow b}, X_{t'+1}^b, X_{t'+2}^b, \dots\}$$

where $a \rightarrow b$ represents a progressive transfer from concept a to b .

- Before $t + 1$, the data is dominated by concept a .
- At $t + 1, t + 2, \dots$, the concept a is shifting to concept b .
- By t' , the data is dominated entirely by concept b .

Figure 2 provides a visualization for the types of drift.

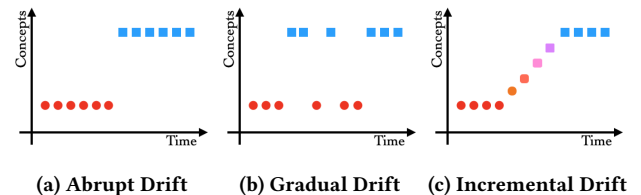


Figure 2: Illustration of Different Concept Drift Rates

Concept drifts can also be regarded as different types based on the “reach of the changing”. A drifting progress can affect feature space, target space, or both. A more detailed explanation of this can be found in [16].

Recurrent drift is a more high-level and complex type of drift. It refers to the phenomenon that a particular distribution could reoccur a certain period [15], where the transition between different distributions can obey any above mentioned drift type.

2.3 Real-World Datasets

The data stream community suffers from the lack of suitable real-world datasets. As criticized by Souza et al. in [28], there are several issues challenging the stream learning with real-world datasets, including difficulty in defining drifts, bias, data stream as an afterthought, etc. These issues become more severe when dealing with regression problems. The data stream regression researchers are still utilizing old and “not-dedicated-to-stream” datasets for evaluating new algorithms [31, 32]. This section introduces some of the datasets relevant to this work.

Abalone [24] is a well-known dataset from the UCI Machine Learning Repository. It contains measurements of physical attributes of abalones, such as length, diameter, weight, and shell dimensions, aimed at predicting the age of the abalones. The Bike Sharing

dataset [5] is a commonly used regression dataset that provides data on bike rental demand, integrating environmental and seasonal settings with temporal features. The House8L dataset [33], derived from the 1990 U.S. Census, is designed for regression tasks aimed at predicting the median house prices in various regions. The Superconductivity dataset, presented by Hamidieh in [17], contains data for predicting the critical temperature of superconductors based on material properties. Real-time energy price datasets from [30] capture dynamic electricity pricing and consumption patterns in New Zealand. These datasets include real-time pricing, historical trends, and contextual variables like weather and time-of-use, emphasizing the role of real-time analysis in managing energy demand and supply for sustainability and cost-effectiveness. Consistently updated pricing data ensures relevance for research and application.

Table 1 summarizes basic information of the real-world datasets, the \uparrow indicates that the instance amount is growing.

Table 1: Real-World Dataset Overview

DATASET	ACRONYM	# INSTANCE	# FEATURE
Abalone	ABA	4,177	8
Bike Sharing	BIK	17,379	12
House8L	H8L	22,784	8
Superconductivity	SUP	21,263	82
NZ Energy Price	NZEP	34,980 \uparrow	11

3 Problem Definition

Regressive analysis in stream learning focuses on building and maintaining models capable of predicting continuous target variables from evolving data streams. Unlike traditional batch learning, stream learning must accommodate challenges such as real-time processing, limited memory, and concept drifts. Regression tasks aim to provide accurate point predictions for the target variable, which are crucial for decision-making in dynamic environments. Beyond point predictions, stream learning also emphasizes uncertainty quantification through Prediction Intervals (PIs), which define a range within which the true target value is expected to lie with a given confidence level.

3.1 Regression

Regression tasks in data stream learning involve predicting a continuous target variable from an incoming, potentially infinite stream of data. These tasks pose unique challenges, including the need to handle evolving data distributions, limited memory, and real-time processing constraints.

3.1.1 Evaluation Methods. To assess the performance of regression models in a data stream setting, two primary evaluation approaches are commonly used:

Cumulative Evaluation: Cumulative evaluation computes the performance metrics over the entire stream from the beginning up to the current moment. It provides a global measure of the model's

performance and is defined as:

$$\text{Metric}_{\text{cumulative}} = \frac{1}{t} \sum_{i=1}^t f(y_i, \hat{y}_i), \quad (1)$$

where t is the number of observed data points, y_i is the actual value, \hat{y}_i is the predicted value, and $f(\cdot)$ represents the evaluation function, such as mean absolute error.

Prequential Evaluation: Prequential evaluation, also known as interleaved test-then-train, uses a sliding window of the most recent n data points to compute performance metrics. This approach captures the model's adaptability to recent data and is defined as:

$$\text{Metric}_{\text{prequential}} = \frac{1}{n} \sum_{i=t-n+1}^t f(y_i, \hat{y}_i). \quad (2)$$

Here, n is the window size, and the summation considers only the most recent n data points.

3.1.2 Evaluation Metrics. Two commonly used metrics for evaluating regression models in data streams are:

Root Mean Squared Error (RMSE): RMSE measures the average magnitude of errors between predicted and actual values, emphasizing larger errors. It is defined as:

$$\sigma_e = \text{RMSE} = \sqrt{\frac{1}{n} \sum_{i=1}^n (y_i - \hat{y}_i)^2}. \quad (3)$$

RMSE is widely used because it provides an interpretable scale of prediction error, matching the units of the target variable.

Adjusted R^2 : Adjusted R^2 evaluates the proportion of variance explained by the model, accounting for the number of predictors to avoid overfitting. It is defined as:

$$\mathcal{R}_{\text{adj}}^2 = \text{Adjusted } \mathcal{R}^2 = 1 - \left(\frac{(1 - R^2)(n - 1)}{n - p - 1} \right), \quad (4)$$

where \mathcal{R}^2 is calculated as:

$$\mathcal{R}^2 = 1 - \frac{\sum_{i=1}^n (y_i - \hat{y}_i)^2}{\sum_{i=1}^n (y_i - \bar{y})^2}. \quad (5)$$

Here, n is the number of data points, p is the number of predictors, and \bar{y} is the mean of actual values.

RMSE is selected because it penalizes larger errors, which are critical in regression tasks, especially in applications where large deviations have significant consequences. Adjusted R^2 is chosen for its ability to measure explanatory power while adjusting for model complexity, ensuring robust evaluation in dynamic data stream scenarios.

3.2 Prediction Interval

Prediction Intervals (PIs) are critical in stream learning scenarios to quantify the uncertainty associated with regression predictions. A PI provides a range within which the true value of the target variable is expected to lie with a specified confidence level. This is particularly important in dynamic data streams where uncertainty may evolve over time.

3.2.1 Evaluation Metrics. Two key metrics are used to evaluate the quality of PIs in stream learning:

Coverage. Coverage measures the percentage of actual target values that fall within the predicted intervals. It evaluates the reliability of the PI and is defined as:

$$C = \text{Coverage} = \frac{1}{n} \sum_{i=1}^n \mathbb{I}(y_i \in [\hat{y}_i^L, \hat{y}_i^U]), \quad (6)$$

where n is the number of data points, y_i is the actual value, $[\hat{y}_i^L, \hat{y}_i^U]$ represents the lower and upper bounds of the prediction interval for the i -th observation, and $\mathbb{I}(\cdot)$ is an indicator function that equals 1 if the condition is satisfied and 0 otherwise.

Normalized Mean Prediction Interval Width (NMPIW). NMPIW evaluates the sharpness of the PIs by measuring their average width, normalized by the range of the actual values. It is defined as:

$$W_{norm} = \text{NMPIW} = \frac{1}{nR} \sum_{i=1}^n (\hat{y}_i^U - \hat{y}_i^L), \quad (7)$$

where R is the target values range: $R = \max(y) - \min(y)$.

The combination of Coverage and NMPIW is essential for a balanced evaluation of PIs. Coverage ensures that the intervals capture the true target values with high reliability, while NMPIW evaluates the precision and sharpness of the intervals. Using both metrics simultaneously ensures that the intervals are neither overly wide (leading to poor precision) nor too narrow (resulting in low reliability). This trade-off is crucial for robust and meaningful uncertainty quantification in dynamic stream learning environments.

4 Related Works

Regressive analyses have always been overlooked in Machine Learning field, not to mention the contempt for the streaming scenario. Novel research on regression and prediction intervals is limited in the recent literature. We choose some new and commonly used algorithms as demonstration tools in this work.

One of the most famous streaming regression models is the Fast Incremental Model Tree with Drift Detection (FIMT-DD) [20]. FIMT-DD incrementally constructs regression trees by splitting nodes based on variance reduction, using adaptive sliding windows to detect and respond to concept drift, ensuring timely updates to the model structure. The Adaptive Random Forest for Regression (ARF-Reg) [8] algorithm builds an ensemble of regression trees, leveraging online bagging with weighted resampling and drift detection mechanisms to dynamically adapt individual trees or the entire ensemble to changes in data streams. Noticeably, the based learner of ARF-Reg is typically FIRT-DD, a variant of FIMT-DD. FIRT-DD utilizes mean target values from the leaf as the final prediction instead of a model output to avoid overflow problems. The Self-Optimising k-Nearest Leaves (SOKNL) [31] algorithm integrates k-nearest neighbors with ARF-Reg, dynamically selecting optimal leaf nodes based on a dissimilarity measurement between centroids in the leaf and the incoming instances. It also adjusts k-values to enhance prediction accuracy on evolving data streams. Furthermore, a sliding-window k nearest neighbours algorithm is also involved in this work due to its universal usage and surprising effectiveness.

Recently, there are some developments in the streaming Prediction Interval aspect. Sun et al. implemented a streaming version of Mean and Variance Estimation (MVE) method and proposed a novel

Adaptive Prediction Interval (AdaPI) [32] algorithm. The Mean and Variance Estimation (MVE) algorithm is a straightforward method for constructing prediction intervals in regression tasks, operating under the assumption that predictive errors follow a Gaussian distribution. It calculates intervals centered around the predicted value, extending by a factor determined by the inverse Gaussian distribution and the standard deviation of errors. Building upon MVE, the Adaptive Prediction Interval (AdaPI) algorithm introduces a dynamic scaling coefficient that adjusts the interval width based on historical coverage. This adaptive mechanism ensures that the prediction intervals converge towards a user-defined confidence level over time, making AdaPI particularly suitable for streaming data where the underlying data distribution may evolve.

5 Data Simulation

5.1 Augmenting Real World Datasets

As exhibited in Section 2.3, the real-world datasets for regression usually consist of “insufficient” instances. However, in order to perform research according to the streaming protocol, the datasets ought to be at substantial length. Therefore, we leverage the development of the generative model and utilize Generative Adversarial Networks (GANs) [12] to enhance the real-world datasets.

In particular, the real-world datasets were used as the input data source to the Conditional Tabular GANs (CTGANs) [36] from the Synthetic Data Vault (SDV) [25]. With the trained generative model, unlimited amount of data points are available for further use.

In this work, the following parametrization is specified to all generative models: (1) epoch number: 300; (2) batch size: 500; and (3) learning rate for generator and the discriminator: 0.001. The other parameters conform with the default values in SDV. All the parameters can be conveniently tuned in our scripts.

5.2 Synthesizing Concept Drifts

In practice, recognizing and defining concept drifts are quite tricky [1, 28]. Without a distinct definition of concept drifts, simulating them is as well an unclear task.

Particularly, the simulation of incremental drift has been challenging the streaming researchers for over a decade. In the current literature, there are two commonly used incremental simulator: Hyperplane [19] and Radial Basis Function (RBF) [18, 22]. Both of them define the concept with their geometric properties. In the Hyperplane case, it is the flat surface in the high-dimensional space, and RBFs rely on the random centroids in the input space. The incremental drifts are simulated by the constant movements of the plane or centroids [11, 13].

In [28], researchers selected the temperature at the moment of the data collection as the drifting feature. Inspired by this idea, we propose a concept simulation approach that utilizes one of the numeric features from the datasets as the concept defining feature, and exploit drift synthesizing methods on the feature to form different types of drifts.

Initially, a “drifting feature” is selected. We apply a pair-wise correlation test between the target and each feature column on the generated data. Multiple methods are available from statistical and machine learning fields, such as pearson test [26], spearman

test [29], feature importance [35], and so forth. Only numeric features can be candidates as the drifting feature for two reasons: (1) numeric values provides more informativeness than categorical ones; and (2) only with numeric values can we synthesize incremental drifts in the following research.

Next, the datasets are sorted based on the drifting feature and separated into distinct chunks. The number of chunks are decided according to the amount of required concepts. All chunks will have different central values in terms of the drifting feature. Each particular chunk will be used for training a CTGAN, which will be later leveraged as the source of a specific concept.

5.2.1 Abrupt Drift. Simulating abrupt drifts is relatively straightforward. With a specific number of drifts, a proper amount of concepts can also be determined. A data stream with a desired length is generated using the associated CTGAN for each concept. These streams will later be vertically concatenated together in a random order (to avoid drifting trends).

5.2.2 Gradual Drift. The simulation procedure of a gradual drift is a bit more complex. we employ the following procedure:

- (1) Extract the last n instances from the initial concept (C_1) and the first n instances from the subsequent concept (C_2).
- (2) Combine these $2n$ instances from C_1 and C_2 into a single set and apply random shuffling to intermix the instances to construct a drifting period.
- (3) Construct the final data stream by concatenating C_1 , the shuffled $2n$ -instance drift segment, and C_2 .

This process generates a smooth transition between C_1 and C_2 , simulating a gradual drift in the underlying data distribution and repeats until the data stream reaches the desired amount of drifts.

5.2.3 Incremental Drift. The steps for synthesizing incremental drift are similar to gradual ones. However, in step (2), instead of shuffling, the data is sorted based on the values in the drifting feature. The direction of the ordering is determined by the average value difference between the concepts at both ends of the drifting period. To avoid potential information leakage caused by the sorted values in the drifting features, in our work, the drifting feature will be discarded from the datasets. Figure 1 plots the drifting feature and the target values from the original Bike datasets after simulating two incremental drifts with 4000 drift length. Evidently, the drifting feature is arranged in an incremental manner. A similar trend can be faintly observed in the target values, although it is not very prominent. This ensures that the simulated concept drift indeed exists while being difficult to detect straightforwardly.

5.2.4 Special Case for NZEP. We treated NZEP dataset group differently in this work due to the extra information they provides. Because the price data is collected from scattered locations across New Zealand, the location information can spontaneously distinguish different concepts. Furthermore, the horizon (how many steps ahead of the forecasting) is also a vital factor when abstracting knowledge from the data. Please see the original work [30] for more details. Thus, when simulating abrupt and gradual drifts on the NZEP data, we choose locations along with different horizons

as the concept. Unfortunately, incremental drifts cannot be synthesized on them since these two features, to some degree, also represent categorical information.

5.3 Synthesized Datasets

To demonstrate the outcomes of our work, we present 18 synthesized datasets and list the details in this section.

Please note that since there are countless combinations of the locations and horizons for NZEP datasets, we manually selected four representatives: (1) Auckland, with 4 hours horizon; (2) Hamilton, with 6 hours horizon; (3) Dunedin, with 30 minutes horizon; and (4) Wellington, with 24 hours horizon.

The generation of the datasets is detailed as follows: In general, for abrupt drifts, we created four concepts with a length of 50k with the source data. As a consequence, all the ‘‘abrupt’’ datasets contains 200k instances. In terms of gradual drifts, the concepts are also 50k instances long and the drifting periods are uniformly set to 10k. As afore-explained, incremental drifts are simulated with the entire data source instead of parts of them, the CTGANs associated with incremental drifts are separately trained. The generated incremental datasets have 100k instances, and 2 incremental drifts with drifting period of 20k. In this manner, the datasets are evenly sectored into 5 parts – 3 stable periods and 2 drifting periods. Each location for NZEP data is individually simulated a incremental dataset, and named after the city, i.e., ALK, HAM, WEL, and DUN. Table 2 illustrates overview of the generated datasets.

Table 2: Overview of Synthetic Datasets
Drift Type Notation – A: Abrupt; G: Gradual; I: Incremental

DATASETS	# INSTANCE	# FEATURE	# DRIFTS	TYPE
ABA _{3a}	200,000	8	3	A
ABA _{3g}	200,000	8	3	G
ABA _{2i}	100,000	7	2	I
BIK _{3a}	200,000	12	3	A
BIK _{3g}	200,000	12	3	G
BIK _{2i}	100,000	11	2	I
H8L _{3a}	200,000	8	3	A
H8L _{3g}	200,000	8	3	G
H8L _{2i}	100,000	7	2	I
SUP _{3a}	200,000	82	3	A
SUP _{3g}	200,000	82	3	G
SUP _{2i}	100,000	81	2	I
NZEP _{3a}	200,000	11	3	A
NZEP _{3g}	200,000	11	3	G
AKL	100,000	10	2	I
HAM	100,000	10	2	I
WEL	100,000	10	2	I
DUN	100,000	10	2	I

6 Experiments and Discussion

This section introduces the conducted experiments, exhibits the results, and facilitates associated discussions.

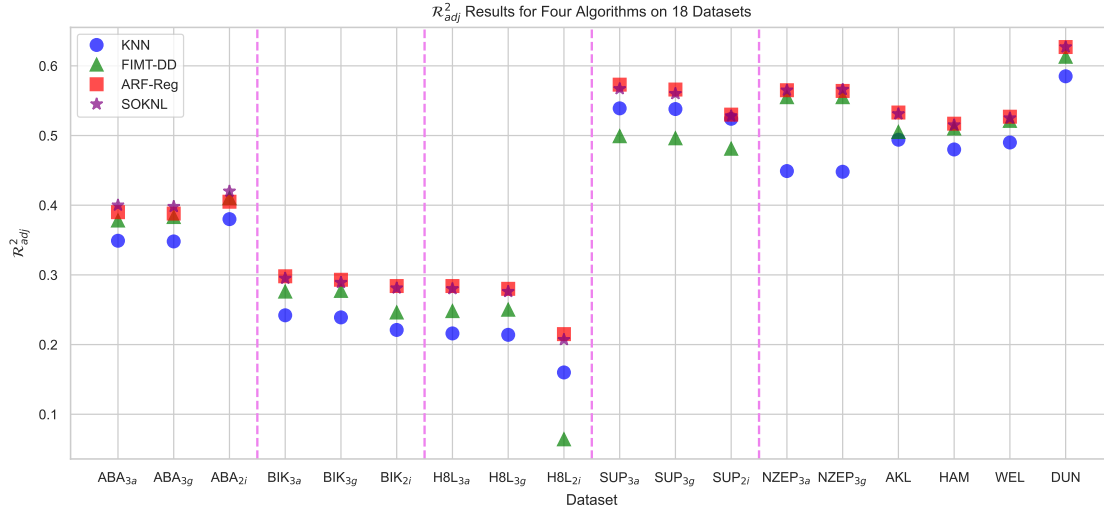


Figure 3: Adjusted R-squared (\mathcal{R}_{adj}^2) Results for Four Algorithms on 18 Datasets

6.1 Algorithms and Parametrization

The following configurations were used to ensure fair comparison and reproducibility: (1) **Sliding Window KNN**: $k = 10$, window size = 1000. (2) **FIMT-DD**: Grace period = 200, split confidence = 0.01. (3) **ARF-Reg** and **SOKNL**: Ensemble size = 30. These settings align with common literature practices and ensure effective performance across datasets. For Prediction Interval experiments, both MVE and AdaPI (Section 4) used a 95% confidence level. AdaPI’s lower limit was set to 0.01, while KNN and SOKNL served as base models with the same configurations. Prequential executions used a window size of 1000. All participants can be located at MOA [1] and CapyMOA, both of which are open-sourced stream learning platforms.

6.2 Regression

Figure 3 compares four regression algorithms – KNN, FIMT-DD, ARF-Reg, and SOKNL – across 18 datasets using their cumulative Adjusted \mathcal{R}^2 (\mathcal{R}_{adj}^2). The x-axis represents the datasets, separated into groups by the vertical pink dashed lines. Each group has the same source of original data, i.e., the first group is derived from Abalone dataset. The standard deviations from ten executions are significantly small, thus omitted in the figure. Because different datasets yield different scale of RMSE (σ_e) results, it is impossible to illustrate all results within a single figure. Therefore, we avoid the illustration for RMSE in the main contents of this paper. Full \mathcal{R}_{adj}^2 and σ_e results can be located in the Appendix (Table 3).

SOKNL and ARF-Reg exhibit comparable performance, both achieving high \mathcal{R}_{adj}^2 values, indicating their accuracy and robustness in streaming regression tasks. While FIMT-DD and KNN perform less effectively, with KNN showing the weakest results overall, the findings suggest that both SOKNL and ARF-Reg are reliable choices for dynamic environments. SOKNL maintains strong stability, while ARF-Reg remains a competitive alternative.

Prequential plots show a more streaming perspective of the results. Due to space restraint, we only illustrate a part of the outcomes here. Figure 4 exhibits the RMSE results on the Abalone dataset group. Apparent sectors can be observed on the “abrupt-drifted” dataset (Figure 4a), while the Figure 4b shows more fluctuations during the drifting periods. The incremental one (Figure 4c) is more turbulent, affirming the effectiveness of the proposed incremental simulation method.

Figure 5 is a prequential \mathcal{R}_{adj}^2 results demonstration for the NZEP dataset group. A key observation is that for the abrupt and gradual (Figure 5a and 5b), only the last concept cause an significant difference. In our case, the fourth concept represents the energy price in Dunedin, which is the only city from the South Island of New Zealand. This indicates a potential difference in the pricing strategy between North (AKL, HAM, and WEL) and South Island (DUN). In terms of the incremental ones (Figure 5c – 5f), they all illustrate different degrees of instability due to the incremental simulated with the most correlated feature to the target values.

6.3 Prediction Interval

Figure 6 and 7 present the cumulative coverage (C) and normalized mean prediction interval width (\mathcal{W}_{norm}) results for different datasets, comparing the performance of MVE and AdaPI methods with kNN and SOKNL models. A tabular result summarization of the cumulative C and \mathcal{W}_{norm} is situated at Table 5 in the Appendix.

Across most datasets, AdaPI consistently achieves higher coverage (C) than MVE, indicating more reliable prediction intervals at a 95% confidence level. However, this increased reliability comes at the cost of wider intervals (\mathcal{W}_{norm}), as seen in datasets like ABA_{3a} and SUP_{3a}. The SOKNL model generally performs better than kNN in terms of narrower prediction intervals (\mathcal{W}_{norm}) while maintaining competitive coverage (C). Notably, the NZEP datasets exhibit excellent coverage and relatively low interval widths, suggesting

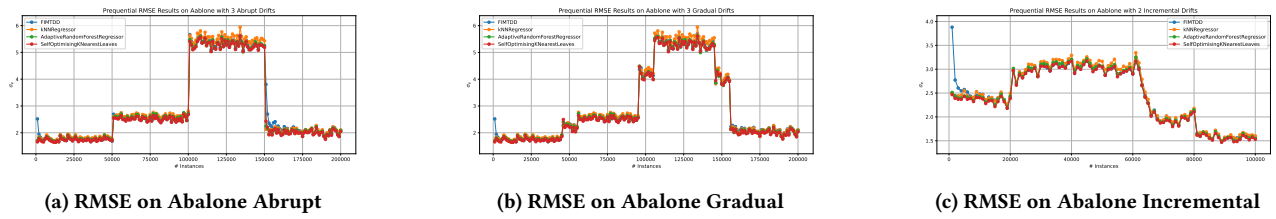


Figure 4: Prequential RMSE (σ_e) Results for Abalone Dataset Group

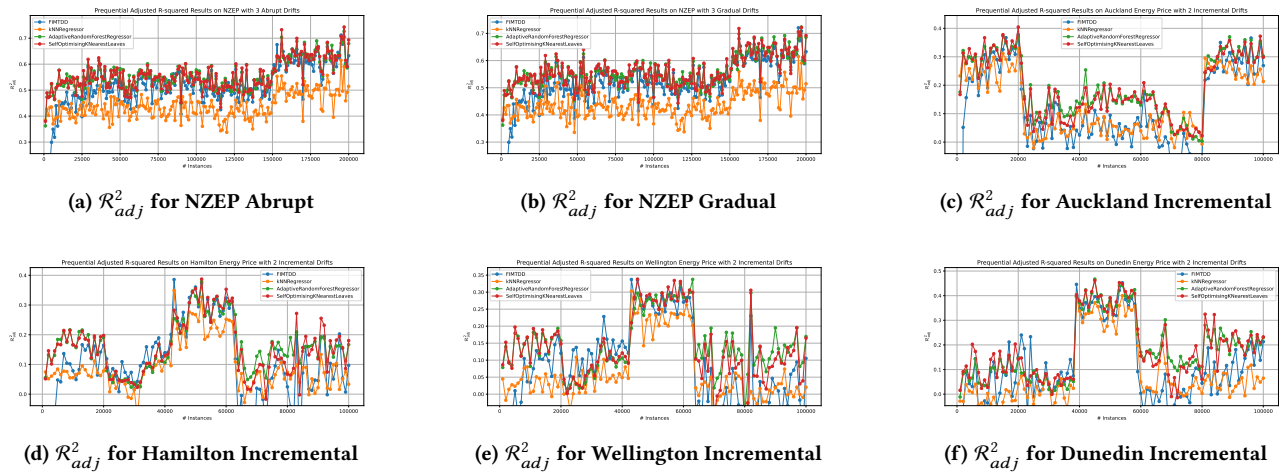


Figure 5: Prequential Adjusted R-squared (R^2_{adj}) Results for NZEP Dataset Group

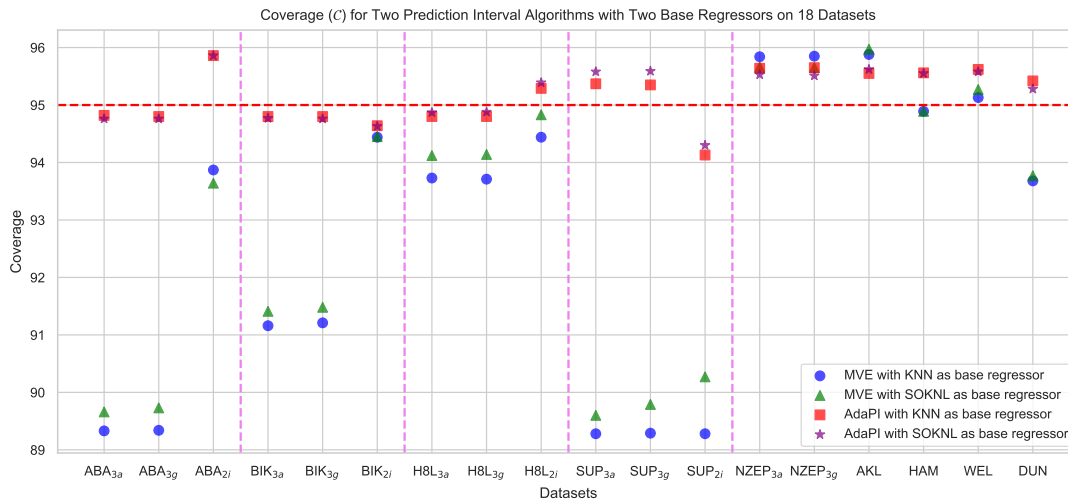


Figure 6: Coverage (C) for Two Prediction Interval Algorithms with Two Base Regressors on 18 Datasets

these methods perform well on energy pricing data. Overall, the results highlight the trade-off between interval width and coverage, with AdaPI and SOKNL offering a balanced and reliable approach.

Figure 8 illustrates the prequential Coverage and NMPIW sequences for MVE and AdaPI (with KNN as the base regressor) on

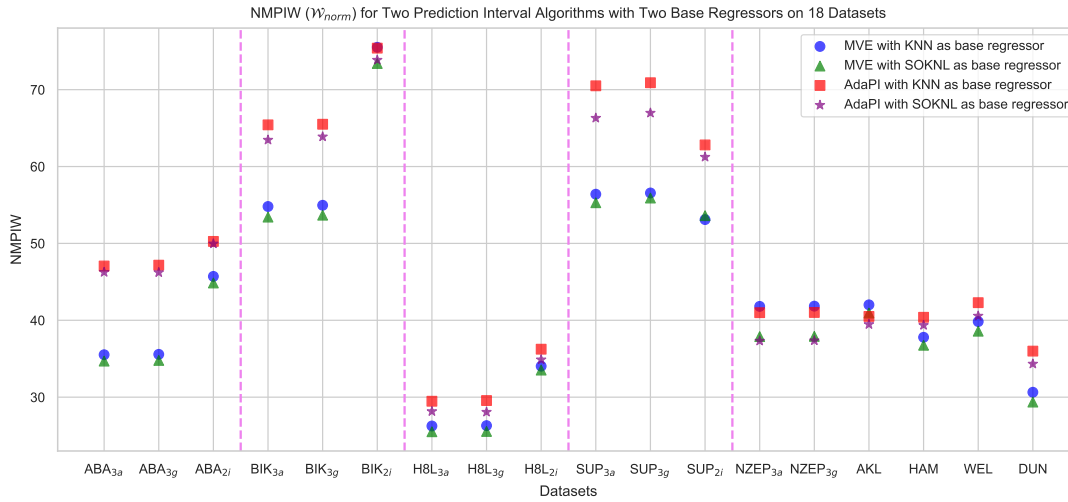


Figure 7: NMPIW (W_{norm}) for Two Prediction Interval Algorithms with Two Base Regressors on 18 Datasets

the House8L Abrupt (H8L_{3a}) dataset. Three drifts are clearly identifiable, with the second drift causing the most significant impact. Using this as an example, we can analyze the following behavior:

After encountering the second drift, the KNN struggles to represent the new concept, leading to a loss of accuracy. In response, AdaPI attempts to recover Coverage by widening the generated intervals to capture more ground truths. Consequently, the NMPIW for AdaPI becomes noticeably larger than that of MVE, as depicted in Figure 8b. The outcome is reflected in Figure 8a, where the Coverage for AdaPI regains the 95% at a faster pace.

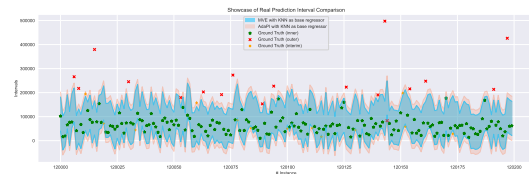
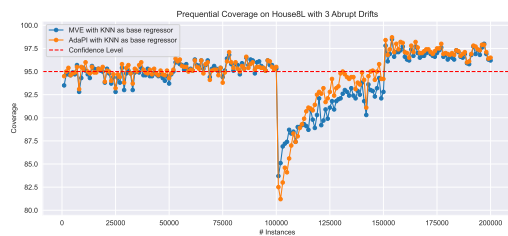
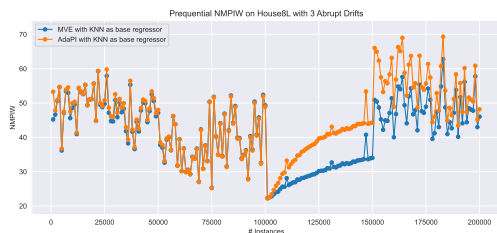


Figure 9: A Clip of the Prediction Interval generated by MVE and AdaPI (from 120,000 to 120,200)



(a) Prequential Coverage (Confidence Level as Red Dashed Line)



(b) Prequential NMPIW

Figure 8: Prequential Coverage (C) and NMPIW (W_{norm}) for MVE and AdaPI with KNN as the base regressor on H8L_{3a}

If we take a more focus look into the streaming progress, as demonstrated in Figure 9, which is a clip of the entire stream of the generated PI areas, it can be spotted that AdaPI (red shadowed region) is larger than the MVE (blue shadowed region) and covers more target values (the orange “+” symbols). This behaviour makes sure that the coverage recovers to the desired values more rapidly.

7 Conclusions

This paper addresses the critical gaps in stream learning research by focusing on regression tasks, which have been largely overshadowed by classification studies. We provide a comprehensive framework for evaluating streaming regression algorithms, highlighting the importance of standardized procedures and well-defined metrics. Our methodologies for simulating concept drifts, especially incremental drifts, using augmented real-world datasets, represent a significant step forward in drift detection and adaptation research.

Through extensive experiments on state-of-the-art algorithms and prediction interval techniques, we demonstrate the efficacy of our framework in analyzing model performance under evolving data distributions. Our results emphasize the need for robust, adaptive methods capable of handling dynamic environments.

Acknowledgments

This research is supported by the TAI AO project CONT-64517-SSIFDS-UOW (Time-Evolving Data Science / Artificial Intelligence for Advanced Open Environmental Science), which is funded by the New Zealand Ministry of Business, Innovation, and Employment (MBIE). URL: <https://taiao.ai>

References

- [1] Albert Bifet, Geoff Holmes, Bernhard Pfahringer, Philipp Kranen, Hardy Kremer, Timm Jansen, and Thomas Seidl. 2010. Moa: Massive online analysis, a framework for stream classification and clustering. In *Proceedings of the first workshop on applications of pattern analysis*. PMLR, 44–50.
- [2] Albert Bifet, Jesse Read, Indrè Zliobaitė, Bernhard Pfahringer, and Geoff Holmes. 2013. Pitfalls in benchmarking data stream classification and how to avoid them. In *Machine Learning and Knowledge Discovery in Databases: European Conference, ECML PKDD 2013, Prague, Czech Republic, September 23-27, 2013, Proceedings, Part I* 13. Springer, 465–479.
- [3] Ajay Choudhary, Preeti Jha, Aruna Tiwari, and Neha Bharill. 2021. A brief survey on concept drifted data stream regression. *Soft Computing for Problem Solving: Proceedings of SocProS 2020, Volume 2* (2021), 733–744.
- [4] Pedro Domingos and Geoff Hulten. 2000. Mining high-speed data streams. In *Proceedings of the sixth ACM SIGKDD international conference on Knowledge discovery and data mining*. 71–80.
- [5] Hadi Fanaee-T and Joao Gama. 2014. Event labeling combining ensemble detectors and background knowledge. *Progress in Artificial Intelligence* 2 (2014), 113–127.
- [6] Joao Gama. 2012. A survey on learning from data streams: current and future trends. *Progress in Artificial Intelligence* 1 (2012), 45–55.
- [7] João Gama, Indrè Zliobaitė, Albert Bifet, Mykola Pechenizkiy, and Abdelhamid Bouchachia. 2014. A survey on concept drift adaptation. *ACM computing surveys (CSUR)* 46, 4 (2014), 1–37.
- [8] Heitor Murilo Gomes, Jean Paul Barddal, Luis Eduardo Boiko Ferreira, and Albert Bifet. 2018. Adaptive random forests for data stream regression. In *ESANN*.
- [9] Heitor Murilo Gomes and Albert Bifet. 2024. Practical machine learning for streaming data. In *Proceedings of the 30th ACM SIGKDD Conference on Knowledge Discovery and Data Mining*. 6418–6419.
- [10] Heitor Murilo Gomes, Maciej Grzenda, Rodrigo Mello, Jesse Read, Minh Huong Le Nguyen, and Albert Bifet. 2022. A survey on semi-supervised learning for delayed partially labelled data streams. *Comput. Surveys* 55, 4 (2022), 1–42.
- [11] Heitor Murilo Gomes, Jesse Read, and Albert Bifet. 2019. Streaming random patches for evolving data stream classification. In *2019 IEEE international conference on data mining (ICDM)*. IEEE, 240–249.
- [12] Ian Goodfellow, Jean Pouget-Abadie, Mehdi Mirza, Bing Xu, David Warde-Farley, Sherjil Ozair, Aaron Courville, and Yoshua Bengio. 2014. Generative adversarial nets. *Advances in neural information processing systems* 27 (2014).
- [13] Nuwan Gunasekara, Bernhard Pfahringer, Heitor Gomes, and Albert Bifet. 2024. Gradient boosted trees for evolving data streams. *Machine Learning* 113, 5 (2024), 3325–3352.
- [14] Nuwan Gunasekara, Bernhard Pfahringer, Heitor Murilo Gomes, and Albert Bifet. 2023. Survey on Online Streaming Continual Learning. In *IJCAL*. 6628–6637.
- [15] Nuwan Gunasekara, Bernhard Pfahringer, Heitor Murilo Gomes, Albert Bifet, and Yun Sing. 2024. Recurrent concept drifts on data streams. In *Proceedings of the Thirty-Third International Joint Conference on Artificial Intelligence, IJCAI-24*. 8029–8037.
- [16] Nuwan Amila Gunasekara. 2023. *Advanced Adaptive Classifier Methods for Data Streams*. Ph. D. Dissertation. The University of Waikato.
- [17] Kam Hamidieh. 2018. A data-driven statistical model for predicting the critical temperature of a superconductor. *Computational Materials Science* 154 (2018), 346–354.
- [18] Rolland L Hardy. 1971. Multiquadric equations of topography and other irregular surfaces. *Journal of geophysical research* 76, 8 (1971), 1905–1915.
- [19] Geoff Hulten, Laurie Spencer, and Pedro Domingos. 2001. Mining time-changing data streams. In *Proceedings of the seventh ACM SIGKDD international conference on Knowledge discovery and data mining*. 97–106.
- [20] Elena Ikonomovska, Joao Gama, and Sašo Džeroski. 2011. Learning model trees from evolving data streams. *Data mining and knowledge discovery* 23 (2011), 128–168.
- [21] Jonathan Jakob, André Artelt, Martina Hasenjäger, and Barbara Hammer. 2022. SAM-kNN regressor for online learning in water distribution networks. In *International Conference on Artificial Neural Networks*. Springer, 752–762.
- [22] Michał Kozłowski, Bartosz Krawczyk, and Michał Woźniak. 2017. Radial-based approach to imbalanced data oversampling. In *Hybrid Artificial Intelligent Systems: 12th International Conference, HAIS 2017, La Rioja, Spain, June 21-23, 2017, Proceedings* 12. Springer, 318–327.
- [23] Shanmugavelayutham Muthukrishnan et al. 2005. Data streams: Algorithms and applications. *Foundations and Trends® in Theoretical Computer Science* 1, 2 (2005), 117–236.
- [24] Warwick Nash, Tracy Sellers, Simon Talbot, Andrew Cawthorn, and Wes Ford. 1995. Abalone. UCI Machine Learning Repository. DOI: <https://doi.org/10.24432/C55C7W>.
- [25] Neha Patki, Roy Wedge, and Kalyan Veeramachaneni. 2016. The Synthetic data vault. In *IEEE International Conference on Data Science and Advanced Analytics (DSAA)*. 399–410. <https://doi.org/10.1109/DSAA.2016.49>
- [26] Karl Pearson. 1896. VII. Mathematical contributions to the theory of evolution.—III. Regression, heredity, and panmixia. *Philosophical Transactions of the Royal Society of London. Series A, containing papers of a mathematical or physical character* 187 (1896), 253–318.
- [27] Jesse Read and Indre Zliobaitė. 2023. Learning from data streams: An overview and update. Available at SSRN 4326595 (2023).
- [28] Vinicius MA Souza, Denis M dos Reis, Andre G Maletzke, and Gustavo EAPA Batista. 2020. Challenges in benchmarking stream learning algorithms with real-world data. *Data Mining and Knowledge Discovery* 34, 6 (2020), 1805–1858.
- [29] Charles Spearman. 1961. The proof and measurement of association between two things. (1961).
- [30] Yibin Sun, Heitor Murilo Gomes, Bernhard Pfahringer, and Albert Bifet. 2024. Real-Time Energy Pricing in New Zealand: An Evolving Stream Analysis. In *Pacific Rim International Conference on Artificial Intelligence*. Springer, 91–97.
- [31] Yibin Sun, Bernhard Pfahringer, Heitor Murilo Gomes, and Albert Bifet. 2022. SOKNL: A novel way of integrating K-nearest neighbours with adaptive random forest regression for data streams. *Data Mining and Knowledge Discovery* 36, 5 (2022), 2006–2032.
- [32] Yibin Sun, Bernhard Pfahringer, Heitor Murilo Gomes, and Albert Bifet. 2024. Adaptive Prediction Interval for Data Stream Regression. In *Pacific-Asia Conference on Knowledge Discovery and Data Mining*. Springer, 130–141.
- [33] Luis Torgo. 1990. House8L Dataset. Derived from the U.S. Census, 1990. Available at <https://www.dcc.fc.up.pt/~ltorgo/Regression/census.html>.
- [34] Scott Wares, John Isaacs, and Eyad Elyan. 2019. Data stream mining: methods and challenges for handling concept drift. *SN Applied Sciences* 1 (2019), 1–19.
- [35] Maksymilian Wojtas and Ke Chen. 2020. Feature importance ranking for deep learning. *Advances in neural information processing systems* 33 (2020), 5105–5114.
- [36] Lei Xu, Maria Skoularidou, Alfredo Cuesta-Infante, and Kalyan Veeramachaneni. 2019. Modeling tabular data using conditional gan. *Advances in neural information processing systems* 32 (2019).

A Appendix

We provide supplementary information to the main contents of the paper.

A.1 Regression

Table 3: RMSE (σ_e) and Adjusted \mathcal{R}^2 (\mathcal{R}_{adj}^2) Results for 18 Datasets

DATASET	METRIC	KNN	FIMT-DD	ARF-REG	SOKNL
ABA _{3a}	σ_e	3.351 ± 0.0	3.274 ± 0.015	3.244 ± 0.001	3.217 ± 0.001
	\mathcal{R}_{adj}^2	0.349 ± 0.0	0.378 ± 0.006	0.39 ± 0.0	0.4 ± 0.0
ABA _{3g}	σ_e	3.353 ± 0.0	3.262 ± 0.015	3.248 ± 0.001	3.222 ± 0.001
	\mathcal{R}_{adj}^2	0.348 ± 0.0	0.383 ± 0.006	0.388 ± 0.0	0.398 ± 0.0
ABA _{2i}	σ_e	2.559 ± 0.0	2.496 ± 0.011	2.506 ± 0.001	2.475 ± 0.001
	\mathcal{R}_{adj}^2	0.38 ± 0.0	0.41 ± 0.005	0.405 ± 0.001	0.42 ± 0.0
BIK _{3a}	σ_e	162.769 ± 0.0	159.073 ± 0.406	156.659 ± 0.071	157.008 ± 0.059
	\mathcal{R}_{adj}^2	0.242 ± 0.0	0.276 ± 0.004	0.298 ± 0.001	0.295 ± 0.001
BIK _{3g}	σ_e	163.056 ± 0.0	158.986 ± 0.277	157.252 ± 0.069	157.599 ± 0.079
	\mathcal{R}_{adj}^2	0.239 ± 0.0	0.277 ± 0.003	0.293 ± 0.001	0.289 ± 0.001
BIK _{2i}	σ_e	182.097 ± 0.0	179.129 ± 2.141	174.468 ± 0.094	174.865 ± 0.069
	\mathcal{R}_{adj}^2	0.221 ± 0.0	0.246 ± 0.018	0.284 ± 0.001	0.281 ± 0.001
H8L _{3a}	σ_e	41320 ± 0.0	40473 ± 418	39503 ± 16	39620 ± 26
	\mathcal{R}_{adj}^2	0.216 ± 0.0	0.248 ± 0.016	0.284 ± 0.001	0.28 ± 0.001
H8L _{3g}	σ_e	41385 ± 0.0	40436 ± 382	39615 ± 9	39722 ± 28
	\mathcal{R}_{adj}^2	0.214 ± 0.0	0.25 ± 0.014	0.28 ± 0.0	0.276 ± 0.001
H8L _{2i}	σ_e	50412 ± 0.0	53117 ± 3625	48724 ± 34	48975 ± 21
	\mathcal{R}_{adj}^2	0.16 ± 0.0	0.064 ± 0.13	0.215 ± 0.001	0.207 ± 0.001
SUP _{3a}	σ_e	24.658 ± 0.0	25.692 ± 0.298	23.74 ± 0.021	23.894 ± 0.03
	\mathcal{R}_{adj}^2	0.539 ± 0.0	0.499 ± 0.012	0.573 ± 0.001	0.567 ± 0.001
SUP _{3g}	σ_e	24.683 ± 0.0	25.766 ± 0.275	23.928 ± 0.01	24.076 ± 0.023
	\mathcal{R}_{adj}^2	0.538 ± 0.0	0.496 ± 0.011	0.566 ± 0.0	0.56 ± 0.001
SUP _{2i}	σ_e	26.976 ± 0.0	28.173 ± 0.936	26.809 ± 0.043	26.884 ± 0.056
	\mathcal{R}_{adj}^2	0.524 ± 0.0	0.481 ± 0.036	0.53 ± 0.002	0.528 ± 0.002
NZEP _{3a}	σ_e	105.524 ± 0.0	94.828 ± 0.756	93.824 ± 0.088	93.728 ± 0.125
	\mathcal{R}_{adj}^2	0.449 ± 0.0	0.555 ± 0.007	0.565 ± 0.001	0.565 ± 0.001
NZEP _{3g}	σ_e	105.634 ± 0.0	94.869 ± 0.754	93.838 ± 0.081	93.642 ± 0.107
	\mathcal{R}_{adj}^2	0.448 ± 0.0	0.555 ± 0.007	0.564 ± 0.001	0.566 ± 0.001
AKL _{2i}	σ_e	98.68 ± 0.0	97.605 ± 1.145	94.858 ± 0.093	95.013 ± 0.116
	\mathcal{R}_{adj}^2	0.494 ± 0.0	0.505 ± 0.012	0.533 ± 0.001	0.531 ± 0.001
HAM _{2i}	σ_e	97.62 ± 0.0	94.702 ± 0.796	94.041 ± 0.073	94.289 ± 0.149
	\mathcal{R}_{adj}^2	0.48 ± 0.0	0.51 ± 0.008	0.517 ± 0.001	0.515 ± 0.002
WEL _{2i}	σ_e	105.797 ± 0.0	102.502 ± 0.583	101.911 ± 0.064	102.16 ± 0.135
	\mathcal{R}_{adj}^2	0.49 ± 0.0	0.521 ± 0.005	0.527 ± 0.001	0.525 ± 0.001
DUN _{2i}	σ_e	93.587 ± 0.0	90.425 ± 0.528	88.818 ± 0.122	88.809 ± 0.084
	\mathcal{R}_{adj}^2	0.585 ± 0.0	0.613 ± 0.005	0.627 ± 0.001	0.627 ± 0.001

Table 3 compares four regression algorithms – KNN, FIMT-DD, ARF-Reg, and SOKNL – across 18 datasets using RMSE (σ_e) and Adjusted \mathcal{R}^2 (\mathcal{R}_{adj}^2). SOKNL consistently achieves the best performance, with the lowest RMSE and highest \mathcal{R}_{adj}^2 , demonstrating its accuracy and robustness. ARF-Reg closely follows, making it a competitive alternative for dynamic environments. FIMT-DD and KNN perform less effectively, with KNN showing the weakest results overall. These findings highlight SOKNL and ARF-Reg as reliable choices for regression tasks on streaming data, with SOKNL excelling in both stability and predictive power.

Table 4 presents the results with same algorithms and same settings with Table 3 on the original datasets summarized in Table 1.

Comparing with Table 3, we can observe that all the algorithms perform worse on the synthesized datasets, which is what we expected. The simulated datasets should be more difficult to predict than the original data. Furthermore, the additional drifts in the synthesized datasets adds more challenges to the data.

Table 4: RMSE (σ_e) and Adjusted \mathcal{R}^2 (\mathcal{R}_{adj}^2) Results for Original Real Datasets

DATASET	METRIC	KNN	FIMT-DD	ARF-REG	SOKNL
ABA _o	σ_e	2.348 ± 0.0	2.733 ± 0.291	2.984 ± 0.017	2.764 ± 0.020
	\mathcal{R}_{adj}^2	0.501 ± 0.0	0.320 ± 0.150	0.246 ± 0.009	0.312 ± 0.010
BIK _o	σ_e	131.716 ± 0.0	Overflowed	97.691 ± 1.389	98.937 ± 0.681
	\mathcal{R}_{adj}^2	0.472 ± 0.0	Overflowed	0.710 ± 0.008	0.702 ± 0.004
H8L _o	σ_e	39928 ± 0.0	38719 ± 1502	36732 ± 158	36461 ± 210
	\mathcal{R}_{adj}^2	0.429 ± 0.0	0.463 ± 0.042	0.517 ± 0.004	0.524 ± 0.005
SUP _o	σ_e	15.415 ± 0.0	Overflowed	21.649 ± 0.045	21.475 ± 0.136
	\mathcal{R}_{adj}^2	0.797 ± 0.0	Overflowed	0.599 ± 0.002	0.606 ± 0.005
AKL _o	σ_e	95.570 ± 0.0	119.993 ± 21.858	95.294 ± 0.373	94.357 ± 0.816
	\mathcal{R}_{adj}^2	0.637 ± 0.0	0.411 ± 0.012	0.639 ± 0.003	0.646 ± 0.006
HAM _o	σ_e	92.252 ± 0.0	106.714 ± 4.751	90.995 ± 0.280	88.938 ± 0.805
	\mathcal{R}_{adj}^2	0.635 ± 0.0	0.511 ± 0.045	0.645 ± 0.002	0.661 ± 0.006
WEL _o	σ_e	88.085 ± 0.0	Overflowed	82.558 ± 0.207	81.762 ± 0.634
	\mathcal{R}_{adj}^2	0.666 ± 0.0	Overflowed	0.707 ± 0.001	0.713 ± 0.004
DUN _o	σ_e	71.631 ± 0.0	Overflowed	75.425 ± 0.207	77.823 ± 0.589
	\mathcal{R}_{adj}^2	0.785 ± 0.0	Overflowed	0.762 ± 0.001	0.746 ± 0.004

Noticeably, there are several “Overflowed” marks in the table, concentrating on the FIMT-DD algorithm. It refers to the phenomenon where one or a few of the predictions extremely differ from the truths, sabotaging the error-based evaluation procedure in regression tasks. Equation 3 and 4 both include $(y_i - \hat{y}_i)^2$ that can cause the overflow problem. The CTGANs’ synthesizing process fixes this problem as there are no overflows over the 18 generated datasets.

A.2 Prediction Interval

Table 5 presents the cumulative coverage (C) and normalized mean prediction interval width (\mathcal{W}_{norm}) results for different datasets, comparing the performance of MVE and AdaPI methods with kNN and SOKNL models. Across most datasets, AdaPI consistently achieves higher coverage (C) than MVE, indicating more reliable prediction intervals at a 95% confidence level. However, this increased reliability comes at the cost of wider intervals (\mathcal{W}_{norm}), as seen in datasets like ABA_{3a} and SUP_{3a}. The SOKNL model generally performs better than kNN in terms of narrower prediction intervals (\mathcal{W}_{norm}) while maintaining competitive coverage (C). Notably, the NZEP datasets exhibit excellent coverage and relatively low interval widths, suggesting these methods perform well on energy pricing data. Overall, the results highlight the trade-off between interval width and coverage, with AdaPI and SOKNL offering a balanced approach for reliable predictions.

Table 5: Cumulative Coverage (C) and NMPIW (W_{norm}) Results with 95% Confidence Level

DATASET	METRIC	MVE		ADAPI	
		KNN	SOKNL	KNN	SOKNL
ABA _{3a}	C	89.33	89.66	94.82	94.76
	W_{norm}	35.52	34.69	47.06	46.25
ABA _{3g}	C	89.34	89.73	94.80	94.76
	W_{norm}	35.57	34.78	47.17	46.22
ABA _{2i}	C	93.87	93.64	95.86	95.86
	W_{norm}	45.71	44.85	50.26	49.96
BIK _{3a}	C	91.16	91.41	94.80	94.77
	W_{norm}	54.80	53.42	65.42	63.46
BIK _{3g}	C	91.21	91.48	94.80	94.76
	W_{norm}	54.96	53.67	65.50	63.88
BIK _{2i}	C	94.44	94.45	94.64	94.63
	W_{norm}	75.51	73.40	75.40	73.86
H8L _{3a}	C	93.73	94.12	94.80	94.87
	W_{norm}	26.25	25.50	29.47	28.15
H8L _{3g}	C	93.71	94.14	94.80	94.88
	W_{norm}	26.30	25.54	29.56	28.07
H8L _{2i}	C	94.44	94.83	95.29	95.39
	W_{norm}	34.03	33.52	36.24	34.88
SUP _{3a}	C	89.28	89.60	95.37	95.58
	W_{norm}	56.40	55.29	70.50	66.31
SUP _{3g}	C	89.29	89.79	95.35	95.59
	W_{norm}	56.56	55.90	70.90	66.97
SUP _{2i}	C	89.28	90.27	94.13	94.30
	W_{norm}	53.10	53.61	62.81	61.24
NZEP _{3a}	C	95.84	95.66	95.64	95.53
	W_{norm}	41.81	37.88	40.99	37.32
NZEP _{3g}	C	95.85	95.65	95.65	95.51
	W_{norm}	41.84	37.91	41.02	37.36
AKL	C	95.88	95.97	95.55	95.62
	W_{norm}	42.01	40.94	40.50	39.47
HAM	C	94.89	94.89	95.56	95.55
	W_{norm}	37.79	36.75	40.39	39.36
WEL	C	95.13	95.27	95.62	95.58
	W_{norm}	39.83	38.58	42.29	40.57
DUN	C	93.68	93.77	95.42	95.28
	W_{norm}	30.64	29.36	35.99	34.33

Table 6 exhibits the cumulative results for the prediction interval settings on the original real-world datasets.

Table 6: Cumulative Coverage (C) and NMPIW (W_{norm}) Results on Original Real Datasets with 95% Confidence Level

DATASET	METRIC	MVE		ADAPI	
		KNN	SOKNL	KNN	SOKNL
ABA _o	C	94.96	95.40	95.26	95.14
	W_{norm}	33.81	32.34	34.36	31.66
BIK _o	C	88.16	88.93	93.76	93.84
	W_{norm}	39.10	27.78	53.74	36.13
H8L _o	C	95.46	96.14	95.37	95.80
	W_{norm}	32.01	29.60	31.46	28.39
SUP _o	C	96.12	96.05	96.55	96.12
	W_{norm}	39.69	46.26	41.09	46.41
AKL _o	C	97.29	97.64	96.82	97.23
	W_{norm}	6.52	6.05	5.92	5.42
HAM _o	C	97.17	97.64	96.78	97.21
	W_{norm}	6.62	5.87	6.04	5.26
WEL _o	C	96.00	96.66	96.10	96.64
	W_{norm}	6.25	5.54	6.04	5.31
DUN _o	C	95.74	95.69	96.44	96.47
	W_{norm}	5.40	5.43	5.28	5.40